The Structure of Low Frequency Phenomena in the Tropics and Its Interaction with the Extratropics

Peter J. Webster
Department of Meteorology, The Pennsylvania State University, PA 16802 USA
and *Min Dong* (董 敏)
Academy of Meteorological Science, State Meteorological Administration, Beijing 100081, PRC
Received January 15, 1991; revised July 19, 1991

ABSTRACT

The structure of planetary scale low freouency phenomena in the tropics is studied, and an attempt is made to determine its influence and interactions with phenomena at higher latitudes.

In the tropics, it is found that the majority of the variance in the zonal wind structure is made up in wave numbers 1 and 2. During warm events in the Pacific Ocean, when the Southern Oscillation Index is negative, almost all of the variance resides in the gravest mode which undergoes a 40° eastward phase shift. Meanwhile, the second logitudinal mode almost disappears. On the other hand, the meridional wind field possesses maximum amplitude at higher wave numbers. However, near the equator,the amplitude is small with extreme values occurring in the subtropics. The difference in scale and the location of extrema of the meridional and zonal wind components indicate that the tropical atmosphere is responding to two different driving mechanisms.

Correlation analyses between variations of the zonal wind at reference points along the equator with variations of component elsewhere show that there are strong logitudinal connections. The strongest correlations between the tropics and higher latitudes exist in the region of the equatorial westerlies. In fact, stronger correlations occur between variations in U anywhere along the equator and the middle latitudes to the north and south of the equatorial westerlies than to the latitudes immediately to the north and south of the reference points. We interpret this "remote" correlation pattern as indicating a two–stage teleconnection process which emphasizes the importance of the equatorial tropical westerlies of the Pacific Ocean as a "corridor" of communication between the low and high latitudes. The regionality of the correlations confirms, to some extent, recent theoretical development regarding trapped equatorial modes. Finally, time lagged correlations from plus and minus six months between variations of U and OLR indicate that the interactions between the extratropics and low latitudes possess an organized sequence. The extratropical influence appears to propagate into the tropics followed by an eastward propagation along the equator. Finally, a propagation from the tropics to the extratropics in the upper troposphere occurs in the eastern Pacific Ocean. The time–lagged correlation sequence does not appear to be symmetric about the equator.

I. INTRODUCTION

Since the 1960's, through a combination of theoretical, diagnostic and modeling studies there has been a substantial increase in the understanding of the structure of the tropical atmosphere, its elementary physical nature and the interaction between the tropics and extratropical regions.Webster and Chang (1988) have suggested that the slowly evolving basic state of the tropical atmosphere completely determines the characteristics of the transient modes. In regions of negative stretching deformation of the zonal wind component along the equator (i.e., where $U_x < 0$), transient energy tends to accumulate as the Doppler–shifted group speeds of the modes go to zero. Such accumulation regions, existing on the eastern side of the westerly maxima of the upper troposphere are also regions of maximum influence to

higher latitudes. For the reverse influence, the studies of Webster and Holton (1982) contend that the upper–tropospheric equatorial westerlies, which extend across the equator in the vicinity of the East Pacific Ocean, act as a duct through which the extratropical rotational modes can propagate deeply into the tropics and even go further to the mid–latitude of the other hemisphere. Theoretical work by Zhang and Webster (1989) has suggested that the degree of trapping of equatorial modes is determined by the sign of the basic state in the divergent tropical atmosphere and the strength of the shear of the wind field. In the central Pacific Ocean, Zhang and Webster show that an equatorially trapped mode may possess turning latitudes which are poleward of 45° of latitude, compared with about 15° in the tropical easterly regime. The clear message from these studies is that the Pacific Ocean region may have a special significance for the communication between the tropics and the extratropics, and vice versa.

However, there are still some aspects of the structure of low–frequency waves in the tropics and the interrelationship of the tropics and the extratropics that are not fully understood. For example, can a Rossby wavetrain emanate from all regions of the tropics or only from a particular region as suggested theoretically for the subseasonal time scales by Webster and Chang (1988)? How do the El Nino events affect the structure of the low–frequency tropical modes and the interaction of the tropics and the extratropics? Are there low frequency modes or mechanisms of communication with the period longer than 40–60 days? If they exist, what role do they play in the general circulation and in the change of climate?Although some of these questions possess hypotheses with theoretical support, it is important that they should be tested against observations.

In this work, we will use a relatively long data set (17 years) to identify the structure of the low–frequency waves in the tropics and the seasonal and intraseasonal time scale interactions between the tropics and extratropics.

II. DESCRIPTION OF THE DATA

The data sets used in this study originate from the operational tropical objective analyses of the NOAA NMC. They consist of monthly mean values of the zonal and meridional wind components at six vertical levels. Here, we will concentrate on the 200 hPa level. The data is set on a 72×23 Mercator longitude–latitude grid whose spacing is 5° in longitude and ranges in latitude from 5° at the equator to 3.5° at the southern and northern boundaries which are located at 48.1°S / N. The data used in the analysis span the time periods from March 1968 through February 1985 with the exception of October and November 1972.

A complementary data set used in this study is the outgoing long wave radiation (OLR) laid out on the same grid described above. These data span the period of June 1974 through February 1985 with the exception of the period from March to December 1978.

III. SPATIAL CORRELATION OF THE ZONAL WIND COMPONENT

In this section we consider the time correlations of the mean monthly structure first. Fig.1 shows the distribution of the correlation coefficient between U anomalies (U′; the deviation of U from its mean monthly value) at a reference point (150°W, 0°) relative to U′ at all other grid points in the domain. Since the wind data in October and November 1972, are not available, the U′ data used in calculating the correlations are from December 1972 through February 1985, providing a sample of 147 monthly mean fields. If all samples are independent, the 95% confidence correlation coefficient should be equal to or greater than 0.161 which is for 140 degrees of freedom. However, the possibility of significant

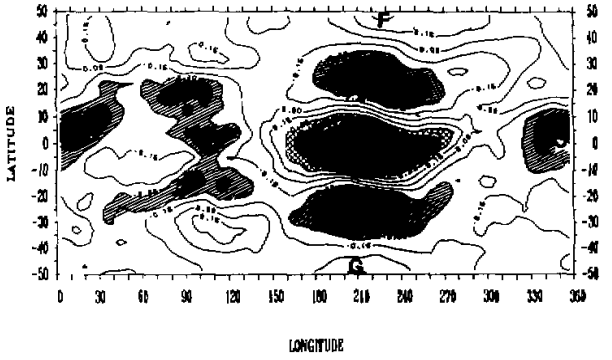

Fig.1. The correlation field of U anomalies at all points with U at the reference point (150°W, 0°N). The contour intervals are at 0, ± 0.16 and the energy ± 0.1. The 95% correlation levels are at ± 0.3. Areas with confidence greater than 95% are shaded or hatched. Various correlation maxima are identified by letters discussed in the text.

autocorrelation in the U′ field series means that there are probably less than 147 independent realizations. Therefore, a calculation of an "effective number of degrees of freedom" of the U′ field was made using Livezey and Chen's (1983) expressions:

$$\tau = \{1 + 2\sum_{i=1} [C_{HH}(i\Delta t)C_{SS}(i\Delta t)]\}\Delta t \tag{1}$$

and

$$n = N\Delta t / \tau \ , \tag{2}$$

where Δt is the sampling time (here equal to one month), N is the number of samples (147), and the C′ s are the autocorrelations at lagsi Δt for U′ at (150°W, 0°; H) and at all other grids (S), respectively. τ is the integrated time scale and n the effective number of degrees of freedom. The minimum number of independent realizations, then, for all grids is 42 which corresponds to a correlation coefficient at the 95% level of 0.3044 for 40 degrees of freedom. Thus, we refer to the grids with correlation greater than or equal to 0.30 as significant at the 95% level. Statistically significant areas in all subsequent diagrams are shaded or hatched.

There are several major significant correlation areas in the tropics and middle latitudes. These are labeled as A, B, C, D and E. In the tropical region, the most significant positive correlation is located in the neighborhood of the reference point (point A). A large negative region is located in the area between 30°W and 125°E (B and C). These correlation patterns along the equator infer that the variations of the zonal winds in the central–eastern Pacific are out of phase with the winds in the Atlantic and Indian Oceans, a phase difference that varies coherently with time along the equator. In the meridional direction of the reference point there are also two significant correlation areas (negative) located to the north and south in the extratropical region around 140°W, 20–30°N / S(D, E) and indications of a pair of areas (positive) even further poleward. We will discuss the correlation between the tropics and the extratropics (i.e., D and E) in Section 5.

If we move the reference point to other longitudes, we can obtain maps similar to Fig.1. Fig.2 shows the correlations between reference points 30° of longitude apart around the equator between 20°N and 20°S (black dot refers to the correlation reference point) and other

grid points in the tropics. It is apparent that at almost all reference points along the equator, the correlation patterns are similar with maxima and minima separated by about half of the equatorial circumference. However, the most impressive negative correlation occurs between central–eastern Pacific and central–eastern Atlantic, i.e., between the regions 150°W–120°W and 0°–30°W.

There are two kinds of significance tests. The first tests for individual (local) significance and the second for field (global) significance. To pass the individual significance test, the correlation between U′ must be equal to or greater than 0.30 for a degree of freedom of 40, as discussed before. However, to pass the global significance test, Livezey and Chen (1983) show that it is required that 12.5% of the total area must pass the 5% individual significance level. Employing this field test, we find that five of the cases shown in Fig.2, specifically when the reference points are located at 0°, 30°W, 120°W, 150°W and 180°, can pass the global significance test, attesting to our visual observation of spatial coherence. Close inspection of the basic field shows that the correlation points possessing global significance are at the points of maximum amplitude of the large scale variability along the equator. The reference points that do not lead to global significance, on the other hand, are at the nodes of the planetary scale variability. To investigate further the correlation patterns, the correlation between the U components at (120°W 0°) and at all other grid points in the equatorial belt (20°N–20°S) for every second month is plotted in Fig.3. Here, each point has a sample number of 17. Since the sampling time interval is one year, their interdependence can be considered rather small, so the degree of freedom of these samples is 15 and the threshold value of correlation of

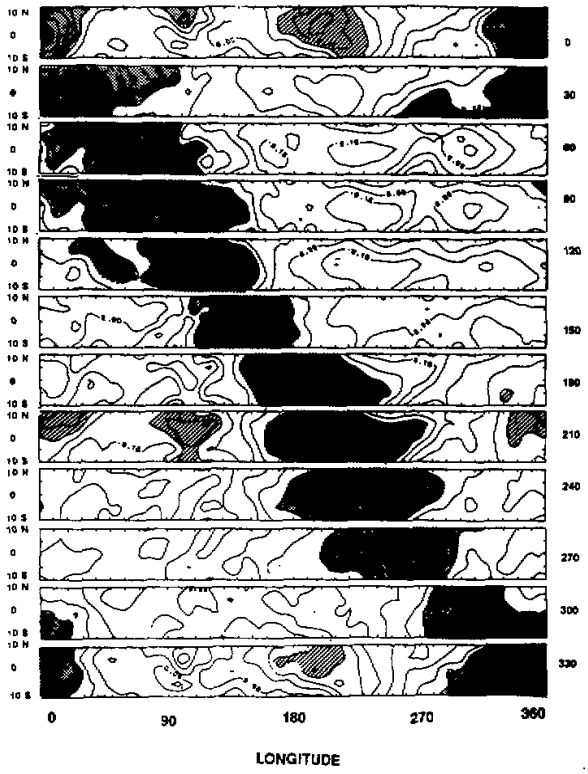

Fig.2. Same as Figure 1 for U at all points with the reference points at successively, (0°E, 0°N), (30°E, 0°N)...(30°W, 0°N). Reference points are marked by black dots.

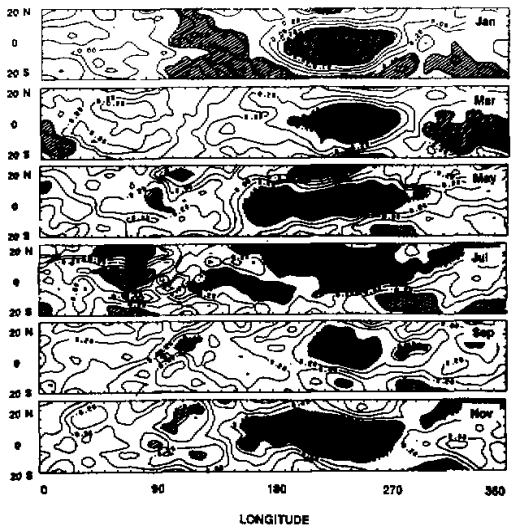

Fig.3. The correlation patterns between U at the reference point (120°W, 0°N) and U at all other grid points for every second month of the year. Shaded regions show correlation greater than 0.48 which is the 95% level.

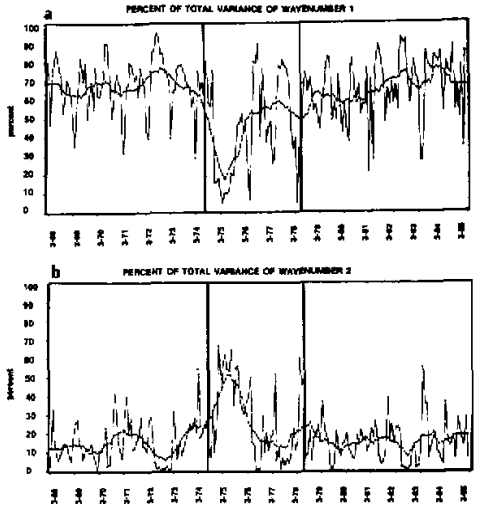

Fig.4. The percentage contribution to the total mean monthly variance of (a) wave number 1, and (b) wave number 2. The dashed line represents a 12-month running average. The vertical lines separate the Cressman, Hough and the Optimal Interpolation Technique initialization schemes.

passing 5% significance test is then 0.48. From Figs.1–3 we can see that the U′ component in the Central–Eastern Pacific Ocean (150°W–120°W) has a strong negative correlation with the

U′ component in the Atlantic Ocean or in the eastern Indian–western Pacific Ocean even on monthly time scales. With the reference point at 150°W for all months except August, the negative correlation region occupies a large area (the area being defined by points where the correlation coefficients greater than 0.48 is above 30) such that they, too, are "globally significant". With the reference point at 120°W, the global significance also holds for most of the year except April, May and November. A common feature for both reference points is that the negative correlations obtain maximum statistical significance in the boreal winter.

In addition to statistical methods, we can use a more direct and simpler technique to verify the result given by correlation analysis. The curves of the mean monthly 200 hPa U component at two locations, the central equatorial Pacific , and the Eastern Atlantic from March 1968 through February 1985 have been plotted (figure omitted). The locations were chosen to reflect the maximum correlations shown in Figs.2 and 3. Overall, most of the anomalies of U at each location appear to be of opposite sign over the entire sampling period. This confirms that the results shown in Figs. 1–3 represent a "general" variability of U′ over the entire period rather than the result just for a few large amplitude events.

IV. STRUCTURE OF THE NEAR–EQUATORIAL CIRCULATION

As early as the 1920's, Walker(1923) found a large scale oscillation between the Indian Ocean and the Pacific Ocean. The phenomenon, of course, was the well–known Southern Oscillation,which was confirmed in many studies . From Figs. 2–3 we can conclude that a similar large scale oscillation occurs not only in the sea level pressure field as described initially by Walker, but also in the upper troposphere U′ field in the tropics.

The large–scale structure of U in the tropics can be examined further by harmonic analysis. Fig. 4 shows the percentage contribution of wave number 1 to the total variance along the equator between March 1968 through February 1985. The dashed line shows the annual running average. A remarkable feature of the figure is the general dominance of the gravest mode. The average percents of the variance over the entire period contributed by waves 1, 2 and 3 are 43%, 19% and 9%, respectively. That is to say, on average, the wave 1 contributes almost half of the total variance. In some periods, the variance contribution of wave number 1 can be greater than 80% (e.g., February, 1984).

The statistical significance of the variation contribution of the waves is given by

$$F=\frac{(a_k^2+b_k^2)/2}{[S^2-0.5\times(a_k^2+b_k^2)]/(n-2-1)}\ , \tag{3}$$

where a_k and b_k are the Fourier coefficients for wave number k, S^2 is the variance of the series and F is the F distribution function having a first degree of freedom of 2 and second degree of freedom of $(n-2-1)$ where n is the length of the series which is 72 here. Under the 5% significance level, the threshold value of F function is 3.11. If the F_k of the Kth harmonic wave is equal to or greater than 3.11, then this Kth wave is considered to be significant. Using Eq. (3), it is found that in all months except April 1975 and April 1978, wave 1 passes the significance test. For wave 2, 80% of the months pass the significance test. However, for wave number 3, only 43% are significant. Comparing the contributions to the total variance of the various waves, it is found that in 180 months, wave number 1 dominates; in 20 months, wave number 2 has the largest contribution; and in only two months does wave number 3 dominate.

V. THE El NINO–SOUTHERN OSCILLATION (ENSO) PHENOMENA AND THE STRUCTURE OF THE ZONAL MODES OF THE TROPICS

The Southern Oscillation Index (SOI) is defined as the normalized pressure difference between Tahiti and Darwin. Periods of negative SOI (e.g.,1968–1969, 1972–1973, 1977–1978, 1982–1983) correspond to warm events in the tropical Pacific Ocean. Bjerknes (1969) related

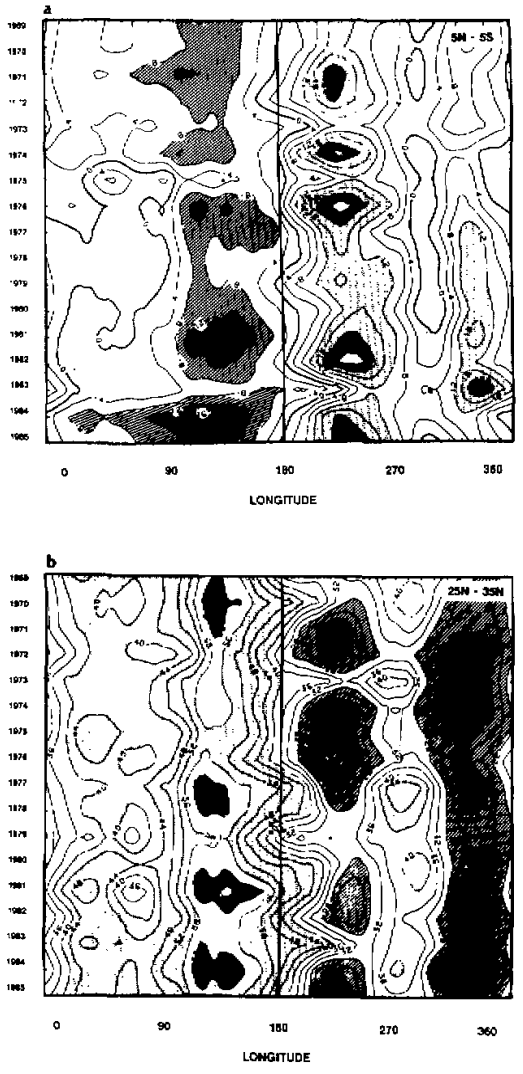

Fig.5. Time–longitude plots of the 200 hPa DJF U component for the latitude bands (a) 5°N–5°S, (b) 25°N–35°N. Regions where $20 < U < 40$ ms are lightly shaded and where $U > 60$ ms are heavily shaded. Heavy line in (a) represents the $U = 0$ contour. Regions where $U > -12$ ms are stippled.

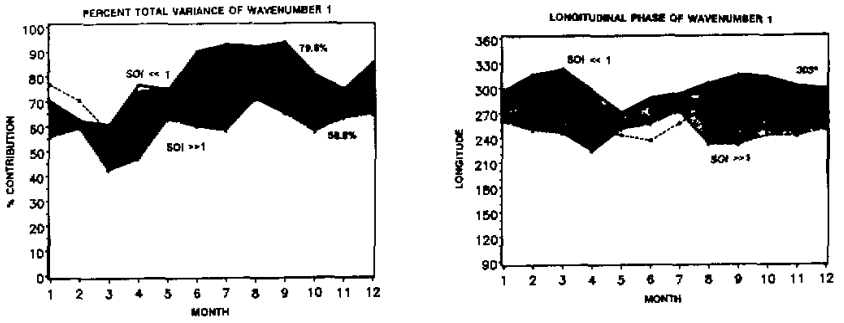

Fig.6. Percentage contribution (upper panel) of wave number 1 to the total variance throughout an El Nino year (SOI $\ll$ 1: solid line), a La Nina year (SOI $\gg$ 1: light–dashed) and normal year (SOI $\approx$ 0: heavy dashed). Longitudinal phase is shown in the lower diagram. Annual variance and phase is indicated on the diagrams.

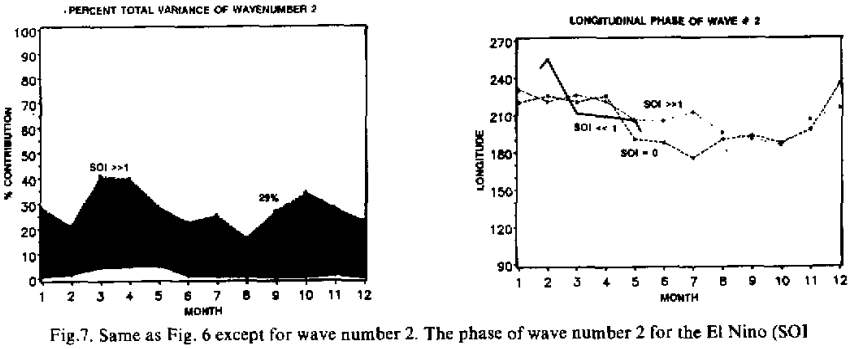

Fig.7. Same as Fig. 6 except for wave number 2. The phase of wave number 2 for the El Nino (SOI $\ll$ 1) year is meaningless given the very low magnitude. Hence the curve is omitted for most months.

the Southern Oscillation Index of Walker to the variation of the sea surface temperature in the Pacific Ocean, defining, thus, the Southern Oscillation–El Nino (ENSO) phenomena. Dynamic quantities are also related to the cycle. Figs. 5a, b show time–longitude sections of the boreal winter (DJF) zonal velocity component in the latitude bands (a) 5°N–5°S and (b) 25°N–35°N over the period of 1969–1985. Since the evolution of zonal velocity in 25°S–35°S is similar to Fig.5b, so it is not given here.

Fig. 5a shows a dramatic variation of the upper tropospheric zonal winds over the eastern Pacific Ocean. During warm event periods in the Pacific Ocean, the winds reduce to weak westerly or even easterly. During "cold events" (i.e., SOI >0 when the western Pacific Ocean is slightly warmer than average in the west and cooler in the east), the winds are very strong and westerly. However, the corresponding variations at higher latitudes in both hemispheres are out–of–phase with the equatorial variations. For example, the periods of strongest equatorial westerlies are matched with weaker westerlies (and vice versa) at higher latitudes.

In order to understand the impact of the warm events on the structure of equatorial waves, the annual variations of the amplitude of wave numbers 1 and 2 for composite annual cycles were calculated. The first composite type relates to an annual cycle during warm events

or periods of large negative Southern Oscillation Index (i.e., SOI $\ll 0$); the second composite relates to the annual cycle with intermediate values of SOI (SOI ≈ 0) and the final type belongs to the "cold event" or "La Nina" (SOI $\gg 0$). For each type, three "typical" months were chosen and the amplitudes of the waves averaged. For example, for the January composite of the warm event category, we choose the Januaries of 1983, 1969 and 1970, which possess SOI values of −3.4, −1.4 and −1.2, respectively. Typical cold event Julys, for example, are 1975, 1979 and 1974, with SOI values of 2.1, 1.3 and 1.2 respectively.

Figs. 6a and b show the annual cycle of amplitude and phase of wave number 1 for the three categories. The solid line represents the warm event case, dashed line the intermediate case and the heavy–dashed line denotes the cold event case. The variance contribution for the warm event case is much larger than the two other categories throughout the year except January and February during which the intermediate category is slightly larger. Another distinction among the categories is that the phase of the wave number 1 (i.e., the longitude of the maximum of the wave) in the warm event case is much further to the east compared to the intermediate year or the cold event year. The maxima are located at 303°E (57°W) and 247°E (113°W), respectively. This eastward shift of wave number 1 during the warm event is consistent with the eastward displacement of the thermal forcing as the maximum of sea surface temperature (SST) moves eastward during a warm event.

Table 1. The Amplitude, Phase and Variance Contribution of Wave 1 for El Nino, Normal and La Nina Case. A represents amplitude, P is phase, S is variance. The subscript e, n, l denote El Nino, intermediate and La Nina, respectively

	El Nino SOI $<<0$			Intermediate SOI ≈ 0			La Nina SOI $>>1$		
	A_e	P_e	S_e / S	A_n	P_n	S_n / S	A_l	P_l	S_l / S
JAN	8.67	298.4	70.1	11.10	267.9	76.8	12.47	259.9	55.7
FEB	8.39	317.4	62.6	11.65	278.0	70.2	10.92	249.5	59.1
MAR	6.82	323.9	60.7	7.90	260.1	57.9	7.56	245.8	42.1
APR	3.56	298.7	76.7	5.37	250.2	50.2	5.08	223.6	46.6
MAY	4.01	271.1	74.5	6.11	243.4	75.1	5.01	250.6	62.6
JUN	6.48	288.6	90.3	7.03	237.0	74.0	5.40	256.8	59.9
JUL	7.67	294.1	92.3	7.38	258.1	82.0	3.40	272.2	58.1
AUG	6.83	307.1	91.9	7.84	279.8	84.9	5.24	232.4	70.8
SEP	7.33	316.1	93.8	4.31	295.0	65.1	5.43	231.3	65.1
OCT	4.56	313.8	80.6	5.69	285.8	69.2	6.26	243.5	57.6
NOV	5.46	303.5	74.9	7.89	272.9	68.4	7.76	242.2	63.1
DEC	8.17	299.5	85.6	8.13	272.8	68.0	10.22	250.3	64.5
Mean	6.50	302.7	79.6	7.50	266.7	70.2	7.06	246.5	58.8

Important differences between warm and cold event years are also apparent in the amplitude and phase of wave number 2. The composite properties of wave number 2 (calculated using the same months as for wave number 1) are shown in Fig. 7. During the warm event year the amplitude of wave number 2 is very small, making negligible contribution to the total variance. During intermediate and cold event years, on the other hand, the amplitude contributions of wave number 2 are much larger, contributing, on average, 20% and 29% to the total variance. Using Eq.(3) to test the statistical significance of wave number

2, we find that during a warm event, no month can pass the 5% significance level test. That is to say during the warm event year there is little evidence of a wave number 2 in the equatorial region. In the intermediate year all months except January pass the 5% significance test while in cold event years all months pass the 1% significance level test. Fig. 7b shows that the phase of wave number 2 for cold and intermediate years is about 150°W. As the amplitudes of wave number 2 during the warm events are statistically insignificant, its phase has no real physical meaning and it is omitted in most composite months of Fig.7. Table 1 provides a summary of the annual cycle of wave number 1 for the La Nina, El Nino and intermediate years.

IV. CORRELATIONS BETWEEN THE TROPICS AND MID-LATITUDES

In Fig. 1 we noted the existence of two large statistically significant negative correlation areas (marked by the letters D and E) with central values of −0.640 (29°S, 140°W) and −0.568 (24°N, 140°W), respectively. On the poleward sides of the negative correlation areas D and E there are two further positive correlation regions (F and G) although their maximum values are somewhat smaller. Thus, in the eastern Pacific Ocean, from the Southern Hemisphere across the equator to the extratropics of the Northern Hemisphere, the sign of the correlations alternates. This correlation pattern suggests that there exists wave propagation from the tropics to high latitudes (or reverse) with a lateral modal scale of roughly 40°to 50°of latitude. Alternatively, one may think of the pattern as representing the latitudinal structure of regionally extended trapped equivalent modes (Chang and Webster, 1990). These connections are also apparent in the dynamic fields shown in Fig. 5. To study the latitudinal correlation structure, we move the reference point along the equator (c.f., Fig. 2) and examine meridional correlation strip maps as a function of latitude between 50°N and 50°S averaged over 60°of longitude about the particular reference point. Fig. 8a shows the distribution of correlations between U anomalies about the reference point and the 60°longitude average U anomalies at all other grid points to the north and south., The upper panel schematically describes the scheme. The curves represent the local correlations of the U anomalies at (say) point C with those along the local meridian C′−C′. The shaded regions denote statistical significance beyond 95%. Similar patterns appear at all longitudes (i.e., negative correlation between the tropics and high latitudes) although only in the vicinity of the upper tropospheric westerlies (i.e., 150°E to 120°W) are the correlations strong and significant away from the equator. The correlation value for statistical significance as calculated by the methods discussed in Section 3 relates to a point correlation and not a 30°average as shown here. Thus, the shaded areas of Fig.8 are probably an underestimate of the significant regions.

Fig. 8b shows the results of an examination of the "remote" tropical−mid−latitude correlation. Here the correlation of U at a reference point at a particular longitude along the equator with the U variation along a longitude−latitude strip to the north and south of the mid−Pacific westerly maximum, specifically in the band between 180°E and 120°W is plotted. i.e., the strips show the variation of the correlation of (say) point C with the 30° averaged correlations along R′−R′. Strong communication appears to exist in the strips between 30°W and 30°E and the extratropics in the reference zone to the north and south of 120°E even though the reference point and reference zone are removed by 180°of longitude!

In summary, Fig.8 indicates that the correlation between the U−variation along the equator at 0°E is much more strongly coupled with the middle latitudes 180°of longitude removed away from the correlation point than is related to variability immediately to the north and south.

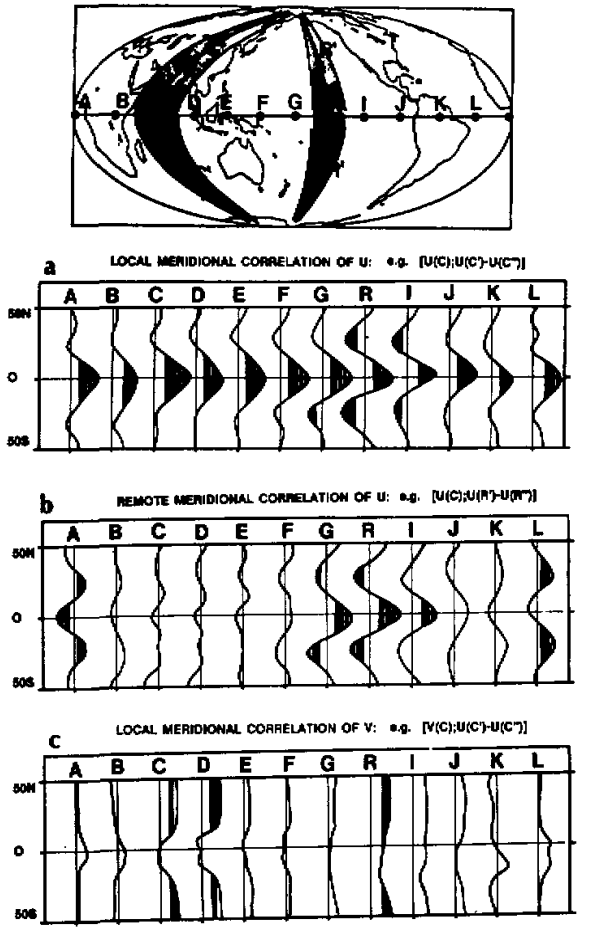

Fig.8. (a) "Local" correlation curves indicating the correlation of U averaged in a 30° longitude strip as a function of latitude for U at the reference points at the indicated longitude (i.e., 0°, 30°E, 60°E,...) and the equator. The correlation scheme is summarized in the map. Shaded parts of the curves denote statistical significance at the 95% level. (b) "Remote" correlation curves indicating the correlation of U averaged in a 30° longitude strip about the 150°W longitude strip relative to the variation of U at the reference points (0°, 0°),(30°E, 0°), (60°E, 0°) ..., and etc.

We also calculated the correlation of V at the reference point (150°W, 0°N), with U at all points for January and the similar correlation map with the reference point at (90°E, 0°N) for July. The correlation patterns indicate the existence of strong, cross equatorial local meridional cell. Figure 8c extends the analysis showing the zonal mean value of the correlation coefficients between the V anomaly (V′) at the tropical reference points (0°, 30°E,...30°W) and the U anomaly (U′) at all points within a 30° longitude belt in a similar manner to the scheme shown in Figs.8a and b. Two areas show significant correlation, at 60°E–90°E and near 150°W. The former is the Asia monsoon region and the second is the equatorial westerly

duct region. The mean correlation coefficient in each region in the mid-latitudes is greater than 0.30.

VII. LAG CORRELATION AND LOW FREQUENCY PROPAGATION

1. *Zonal Velocity*

Lag correlations are useful in revealing the temporal nature of climate. Fig. 9 shows the lag correlation between U′ at (120°W, 0°) with U′ at all other points. A positive lag value indicates that the point (120°W, 0°) leads other grid points. A negative lag value indicates that the reference point lags other points. Latitude–longitude plots of correlation with lags monthly from −6 months to +6 months are shown. Regions of positive correlation (>0.30) are enclosed in the solid shaded contour and significant negative correlations (<0.30) are hatched.

When the lag is −6 months, the significant correlations (designated by A) are located in the western Pacific (145°E–175°E, 0°–10°N) with a maximum positive value of 0.379. As the lag decreases, region A moves eastward and equatorward and increases in value. With the lag at −1 month, the maximum correlation center moves just to the west of the reference point (i.e., 140°W, 0°N) with a value of 0.643. As lag becomes positive (i.e., the reference point now leads other grid points), A moves to the east of the reference points. Although the correlation decreases in statistical significance (smaller than 0.30) with the lag increasing beyond +4 months, we still can trace the slowly eastward movement of the maximum correlation center. In summary, between lags of −6 to lag +6 the correlation center, A, moves slowly eastward over a distance of 150°longitude with an average propagation speed of 10–15° longitude or so per month. Secondary positive maxima (B and C) occur to the south and northeast of A. Although both B and C never attain statistical significance, they follow an orderly and coherent propagation.

An eastward propagation of an opposite sign correlation pattern (Y) also occurs along the equator considerably to the west and is apparent even at −6 months although it does not achieve significance until −5 months. Together with A, the impression is that the correlation pattern migrates along the equator as a wave number one and two system. The propagation suggests that the low frequency signal along the equator originates in the western Pacific / Asian region and propagates eastward. The development of the negative center along the equator coincides with an extended region in the extratropics of both hemispheres (X and Z). Through time, the negative pattern appears as a "Y" shape with the open end facing westward and the vertical arm along the equator. As the lag decreases, the "Y" moves eastward strengthening into distinct correlation centers along the equator and to the north and south of the positive correlation maximum. The negative tongues seem to extend westward and "curl" into the tropics. This occurs at a time (about −3 to −2 months) with the establishment of the negative maximum along the equator (W). The extratropical maxima coincide with the westerly maxima shown in Fig. 5. With positive lags, the extratropical maximum negative correlations continue eastward at a faster rate than the tropical positive maximum. The effect is to reverse the orientation of the negative "Y" pattern which now seems to open to the east.

The results presented in Fig.9 show a systematic temporal structure of the zonal wind. The pattern evolution in the tropics appears to follow that described by Gill and Rasmusson (1985) with a signal emerging from the western Pacific Ocean. Between the extratropics and tropics, the patterns seem to suggest an organized sequence similar to those found by Barnett

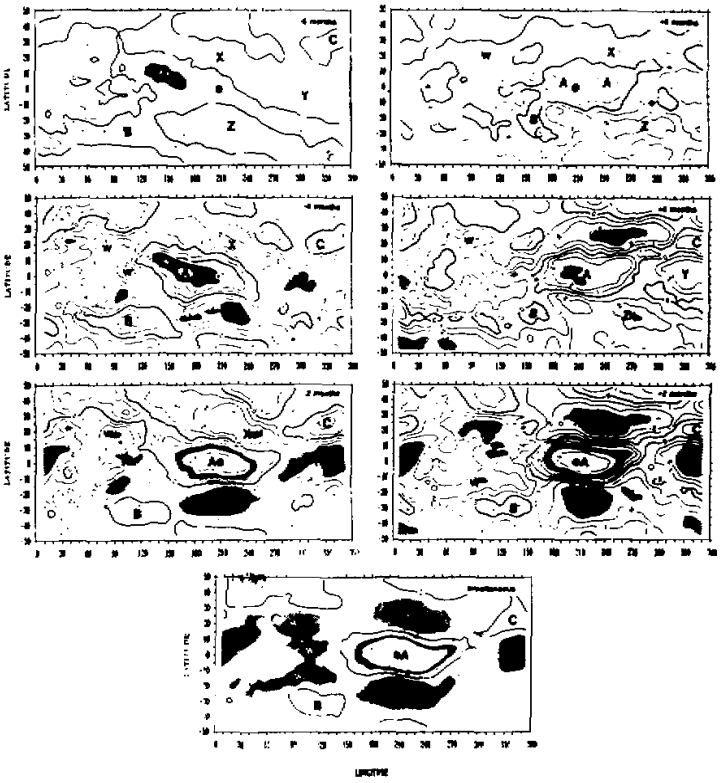

Fig.9. Lag correlations of U at reference point (120°W, 0°) and all the U between ±6 months. Letters refer to correlation pattern centers identifiable from lag to lag. Areas within shading and hatching are statistically significant to 95%.

(1984, 1985) who used more sophisticated statistical techniques than those employed here. Clearly, there are strong lag and lead correlations between circulation variations at low latitudes and the extratropics that require investigation. However, there is a clear and important conclusion that appears to emerge from the analysis. The tropics and the extratropics are certainly connected. Furthermore, the interaction appears to be in both directions. Another observation is that the strongest negative correlations (X and Z) seem to occur in the region to the north and south of the equatorial westerlies which correspond to the Webster and Holton "westerly duct." We note for later reference that it is also a region of minimal longitudinal shear.

2. *The Correlations between OLR and Velocity Potential* (χ)

To understand further the propagation of the large–scale tropical waves and the interactions between the tropics and mid–latitudes, we choose OLR and χ (velocity potential) for a correlation analysis. The velocity potential, χ was calculated using the relationship

$$\nabla^2\chi = \nabla \cdot \mathbf{V} \ , \tag{4}$$

which is solved using an overrelaxation scheme. The OLR can be considered as a proxy for rainfall in the tropics because it is closely linked with the development of convective cloudiness. Thus, minimum OLR areas, representing deep and persistent convective clouds, are usually considered to be related to heating source regions.

The OLR data are only available from June 1974, and as continuous data from only December 1978 which is chosen as the starting date for the calculation of the correlation fields between OLR and χ. Thus, a total of 74 months is available for analysis. Within a 95% significance level, the threshold value of the correlation coefficient is 0.23 when the degree of freedom is 70. However, as discussed previously, there are far fewer degrees of freedom than 70. In fact, the results of calculation based on (3) and (4) show that the average value of effective degree of freedom for 12 reference points (0°, 30°E ··· 30°W) is only 27 so that the critical correlation coefficient at the 95% significant level is 0.368.

Fig.10 shows the simultaneous and lag correlations between −6 and +6 months for the OLR at the reference point (120°E, 0°N) and χ at all other grid points. The reference point was chosen as it represents the center of the mean OLR minimum. The figure clearly reveals a dipole pattern along the equator and a strong connection between the tropics and mid–latitudes, especially in the vicinity of the reference point, and in particular, near 120°W where the

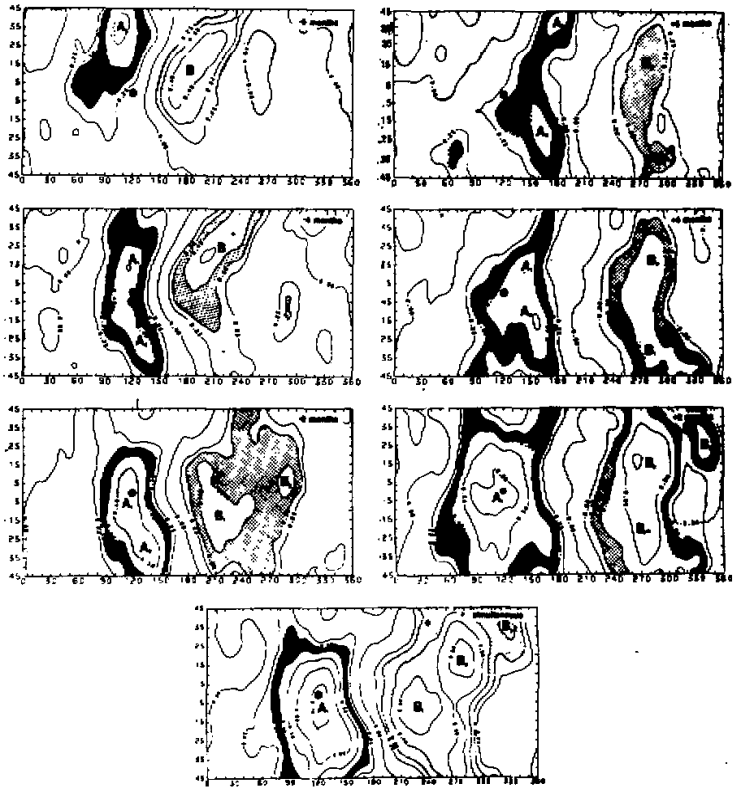

Fig.10. Lagged correlations between ± 6 months for the OLR at (120°E, 0°) with χ elsewhere. Areas in this shading and hatching are statistically significant to 95%. Letters refer to correlation pattern centers identifiable from lag to lag.

upper tropospheric westerlies are strongest.

In the simultaneous correlation map (bottom panel, Fig.10) there are two significant correlation areas. One center is positive (point A maximum value 0.738) and is located in the neighborhood of the reference point, about the equator and around 120°E. The other center is negative (point B), and located near 120°W and the equator. If we can think of negative χ fields as being associated with upward motion, positive correlation regions suggest ascent associated with convection at the reference point. Negative correlations, on the other hand, imply descent resulting from the convection. Thus, the simultaneous correlation patterns suggest that the region which determines the strength of the Walker cell is the convective region of the West Pacific and that the associations are on the largest longitudinal scale. The regional extension of the negative correlation area well to the north and south of the equator indicates the importance of variation in tropical convection intensity to the higher latitudes.

We focus our attention on the positive correlation region in the Asian western Pacific region. At lags of −6 months, the largest correlation (point A) is located at 35°N, 105°E with a maximum value of 0.53. Between lags −4 or −2 months, the significant positive correlation moves towards the equator and slightly to the east. At positive lags, the significant correlations move from the equator to high latitudes in both hemispheres and even further to the east. With the lag at +6 months, there are two significant correlation areas located in 25°S, 165°E (A_1, $r = 0.448$) and 41°N, 180°(A_2, $r = 0.442$), respectively. The movement of significant correlation region with the change of the lag length suggests that variations in the χ−field in the northern and southern western Pacific Ocean precede by several months the variation of convection in the western Pacific Ocean. The negative correlations, on the other hand, follow a similar pattern between lags −6 and −2 months. However, as the lag becomes positive, the negative area (B) occupies most of the Western Hemisphere and extends poleward in both hemispheres. On the other hand, the changes of OLR in the western Pacific precede variations in the extratropics of the northern and southern eastern Pacific Ocean.

In summary, the correlations suggest that there are low frequency associations between the extratropics and the tropics and vice versa. However, the relationships are not symmetric about the equator. For example, the −6 month lag correlation shows that the significant positive area A correlation residing in the Northern Hemisphere has no counterpart in the Southern Hemisphere. Perhaps this asymmetry may be explained by the different geography of the two hemispheres. On the other hand, with positive lags, both the positive and negative patterns appear symmetric about the equator.

The patterns shown in Figs. 9 and 10 are similar to the variations in mean sea level found by Barnett (1985) who noted that a large scale signal propagated along the equator from the monsoon regions to the eastern Pacific Ocean and from there to higher latitudes.

VIII. SUMMARY

From above analysis, the following conclusions have been reached:

(i) In the tropics, the dominant components of the U−field are longitudinal wave numbers 1 and 2. Thus, the variation of the U component in the central eastern Pacific Ocean is out−of−phase with the variation in the Indian and Atlantic Oceans.

(ii) The spectral distribution of the U−field is strongly affected by ENSO events. In an El Nino year , wave 1 provides a much larger contribution to the total variance compared with intermediate or La Nina years . Wave number 2 provides very little contribution to the total variation during an El Nino year although in a La Nina year, it increases its amplitude significantly.

(iii) The ENSO events also change the phases of the low frequency structure of the trop-

ics. In an El Nino year, the anomalous SST distribution in the Pacific Ocean forces the divergent and convergent centers to move eastward with a consequent eastward migration of the phase of wave number 1. On the other hand, in a La Nina year, the phase of wave number 1 shifts westward creating large phase differences ($>50°$ of longitude) between the two extremes.

(iv) Correlations between U' at the equator and U' elsewhere indicate that there are strong latitudinal correlations between the tropics and midlatitudes, especially in the regions of the upper tropospheric equatorial westerlies (of the central and eastern Pacific Ocean). Variations of U in the upper tropospheric easterlies are only weakly correlated with variations to the north and south. In fact, variations in the easterlies are more strongly correlated with the geographically remote variations of U to the north and south of the equatorial westerlies.

(v) The weak local correlation between U' at the equator and U' at higher latitudes in the vicinity of the equatorial easterlies and the much stronger local correlation between V' at the equator and U' elsewhere in the same location suggest the coexistence of two mode forms. The former correlation suggests a dominance of an even or symmetric mode about the equator in U oriented zonally. The latter correlation suggests that the V field at low latitudes is connected to an odd mode about the equator oriented meridionally which is probably part of the Asian monsoon system.

(vi) The lagged correlation fields between OLR and χ reveal that there are strong interactions between the tropics and extratropical regions which, within the limitations of the data, appear to have a definite sequence. An extratropical signal appears to propagate into the tropics. Perhaps because of the differences between the two hemispheres in topography and ocean–land distribution, the tropical–extratropical interactions do not appear to be symmetrical about the equator.

The authors would like to acknowledge the support by the National Science Foundation provided under Grants ATM83–18852 and ATM87–03267. We would like to thank Dr. P.A. Arkin, NOAA for providing the data set used in the study as well as for a number of interesting discussions. We are also indebted to our colleagues Dr. Song Yang and Dr. H.R Chang. We also would like to thank the USA / PRC Bilateral Agreement on monsoon research for the support of Mr. Min Dong during his visit to the United States.

REFERENCES

Arkin, P. A. and P. J. Webster (1985), Annual and interannual variability of tropical–extratropical interaction, *Mon. Wea. Rev.*, **113:** 1510–1523.

Barnett, T. P. (1984), Long–term trends in surface temperature over the ocean, *J. Atmos. Sci.*, **42:** 478–501.

Barnett, T. P. (1985), Variations in new–global sea level pressure, *J. Atmos. Sci.*, **42:** 478–501.

Bjerknes, J. (1969), Atmospheric teleconnections from the equatorial Pacific, *Mon. Wea. Rev.*, **97:** 163–172.

Chang, H.–R. and P. J. Webster (1990), Energy accumulation and emanation at low latitudes. Part II: Nonlinear response to episodic equatorial forcing. *J. Atmos. Sci.*, **47:** 2453–2464.

Gill, A. and E.Rasmusson (1983), The 1982–83 climate anomaly in the equatorial Pacific, *Nature*, **306:** 229–234.

Livezey, R. and W. Y. Chen (1983), Statistical field significance and its determination by Monte Carlo techniques, *Mon. Wea. rev.*, **111:** 46–59.

Walker, G. T. (1923), Correlation in several variations of weatherVIII: A preliminary study of world weather, Vol. 24, Part 4, Superintendent of Government Printing, India, 75–123.

Webster, P. J. and J. R. Holton (1982), Cross–equatorial response to sea surface temperature anomalies, *J. Atmos. Sci.*, **39:** 722–733.

Webster, P. J. and H.–R. Chang (1988), Tropical accumulation and emanation: Wave propagation through a zonally varying basic state, *J. Atmos. Sci.*, **45:** 803–829.

Zhang, C. and P. J. Webster (1989), The mechanics of equatorially Rossby mode trapping, *J. Atmos. Sci.*, **46:** 3632–3652.